COMPARISON OF SIMPLE AND OPTIMIZED ON-OFF CURRENT CONTROLLERS FOR THREE PHASE SYSTEMS

Hans ERTL, Johann W. KOLAR and Franz C. ZACH

Technical University of Vienna - Power Electronics Section
Gusshausstrasse 27-29, A - 1040 Vienna, AUSTRIA

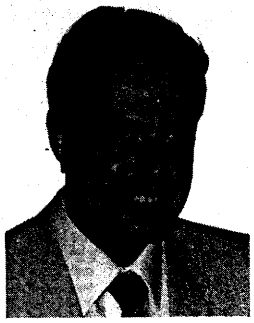

A B S T R A C T

This paper treats the problem of on-off current control for coupling of a DC voltage system with a three phase (polyphase) AC voltage system via a pulse width modulated (PWM) inverter. Thereby the AC voltage represents (according to the direction of the energy flow which is possible in both directions) either the emf of an AC machine or the three phase power supply system (mains).

The following control concepts are investigated by digital computer simulation:

1. a simple hysteresis controller,
2. a predictive controller with on-line optimization (optimization with respect to minimum switching frequency) and
3. a controller based on off-line optimization (using a switching table).

It is shown that for the system analyzed here, the relatively involved (concerning its realization) predictive controller can be replaced by a switching table of very limited size. For rating of the treated controllers the switching frequency (at the same rms value of the current control error) as a function of the rms voltage of the AC system and the other system parameters is used.

1. INTRODUCTION

One of the main areas of interest in power electronics as applied to modern drive systems is the supply of AC machines from a DC voltage link via a PWM converter. Basically in such cases a DC system is coupled with the polyphase AC system (for the sake of brevity from here on only called three phase system) generated by this converter. The converter can be regarded as a "transformer" with the inherent ability for a bidirectional energy flow between the two voltage systems [1]. The reversed energy flow (i.e., from the AC side to the DC side) leads to a structure called Forced Commutated Rectifier, FCR [1]. Also the drive system mentioned earlier only represents an application of a general power electronic system for coupling of two voltage systems (DC and AC) which (as shown in Fig.1) for the following can be imagined by ideal AC or DC voltage sources. The basic properties for this structure can be summarized as follows:

* possibility of bidirectional energy flow
* sinusoidal currents on the AC side
* due to the balanced power between AC and DC side the energy storage elements (L and C) have to be dimensioned only with respect to the power pulsating with switching frequency
* no voltage and current distortion on the AC side (in the ideal case)
* definable reactive power consumption (generation)

* decoupling of the AC amplitude and the DC link voltage

* simple converter structure (state of the art)

The main state variables of the described power electronic system with respect to physics and technology are given by the currents of the AC side. This is because they determine the energy flow in the system (considering their phase relationship with respect to the voltage) and the maximum current stress of the switching device. It is therefore obvious that the control concept for the system should incorporate these characteristic variables. In this paper the problem of current control of the mentioned power electronic system is treated exclusively.

In order to limit the extent of this paper only on-off control characteristics are considered. For these the switching instants are asynchronous (i.e., they are not correlated to the period of the AC voltage); this can be explained by the fact that the current is only controlled (guided) within a deadband around its reference value. This results in not exactly defined fundamentals (with regard to amplitude, frequency and phase) of the converter output AC voltage and current. An alternative to this (asynchronous) control concept as treated here is given by application of a pulse pattern generator for which the modulation depth is controlled dependent on the current control error. Then there are possible synchronous as well as asynchronous modi of operation. The former is characterized by a discrete frequency spectrum.

The classical (and simplest) realization of an on-off controller for a three phase system is given by three independent hysteresis phase current controllers. The voltage between the virtual center point of the DC link voltage U_z (I in Fig.1) and the star (neutral) point of the AC system (II in Fig.1) is given by the switching status k_I (k_I = 0..7). The voltage between I and II is u_o = (u_{OR} + u_{OS} + u_{OT})/3 where u_{OR}, u_{OS}, u_{OT} are the phase voltages of the converter with respect to point I. Therefore the change of the switching status of one phase effects the other phases. Because this coupling effect is not a priori considered by the simplest on-off control system as described before, among other properties a maximum current control error of twice the deadband width results.

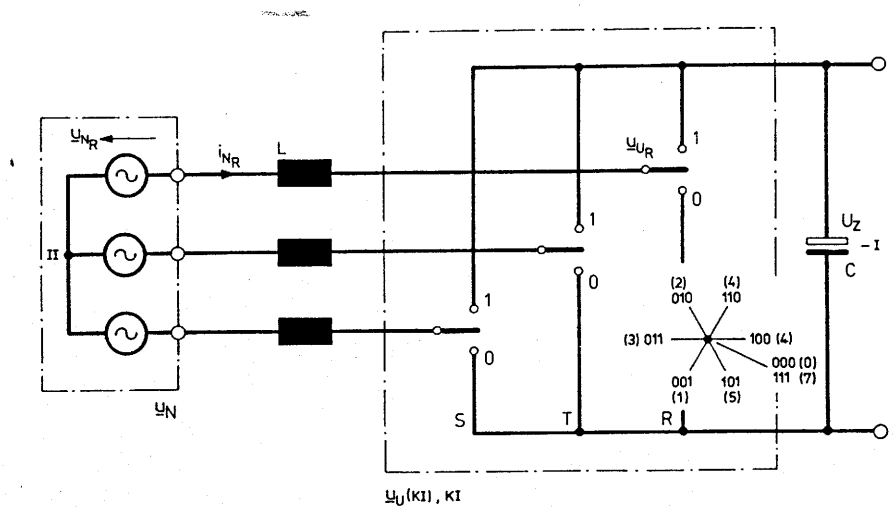

Fig.1 Basic structure of interconnection of an AC and a DC system via a pulse width modulated converter (PWMC). One converter leg (e.g., 2 power transistors with antiparallel freewheeling diodes) can be symbolized by a simple switch connecting either the positive or the negative DC link bar to the respective AC phase. (The switching position shown here is not possible !)

If the switching actions of the different phases are coordinated the current can be kept within the deadband. Furthermore then also an optimization (as described, e.g., in [2]) is possible aiming at a minimum switching frequency; an other optimization criterion is, e.g., minimization of the rms value of the current control error. Because such an optimization basically is only meaningful for stationary operating conditions a second control system has to be superimposed on this optimized controller to handle transient conditions (see sections 4 and 5).

In this paper the stationary operating conditions of a simple on-off controller, of a controller based on off-line optimization (using a switching table) and of an on-line optimizing (predictive) on-off current controller are investigated and compared by digital computer simulation.

2. DESCRIPTION OF THE SYSTEM BY SPACE VECTORS

According to Fig.2 the space vector differential equation is given by

$$\underline{u}_N = \underline{u}_U(k_I) + L \frac{d\underline{i}_N}{dt} \qquad (1)$$

where $\underline{i}_N$ is the AC current (called also mains current in the following), $\underline{u}_N$ is the mains voltage and $\underline{u}_U(k_I)$ is the converter output (AC side) voltage (switching status k_I).

We define

$$\Delta\underline{i}_N = \underline{i}_N^* - \underline{i}_N \qquad (2)$$

as the current control error. This yields with Eq.(1)

$$L \frac{d\Delta\underline{i}_N}{dt} = \underline{u}_U(k_I) - (\underline{u}_N - L \frac{d\underline{i}_N^*}{dt}) = \underline{u}_U(k_I) - \underline{u}_{Ui} \qquad (3)$$

In Eq.(3), $\underline{u}_{Ui}$ represents that (ideal) converter output voltage which on one hand forms the counter voltage to the mains and on the other hand would effect a current change in L according to the reference value change. There are only six different nonzero converter output voltage vectors of equal magnitude (with a direction depending on the switching status k_I)

$$|\underline{u}_U(k_I)| = \frac{2}{3} U_Z, \quad k_I = 1..6 . \qquad (4)$$

Together with both zero vectors $k_I=0$ and $k_I=7$, there exist alltogether

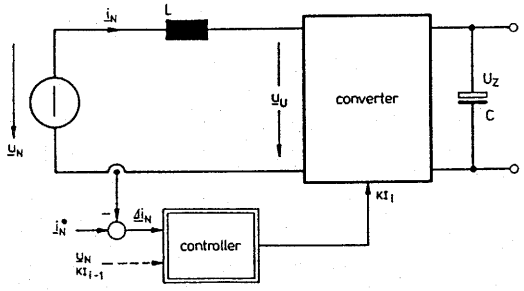

Fig.2 Control structure of the system (Fig.1) based on space vector description of the state variables.

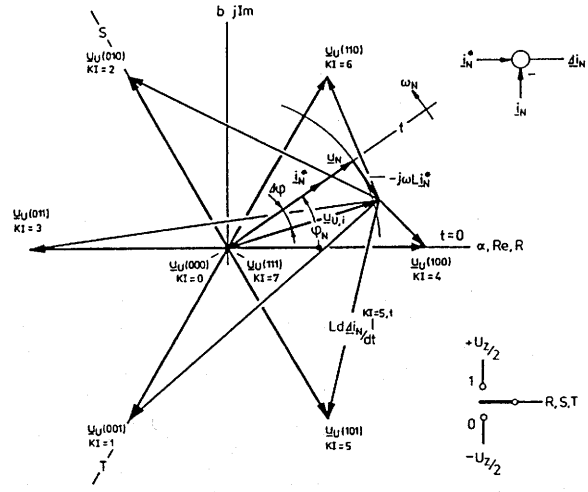

Fig.3 System state vectors

seven vectors $d\Delta\underline{i}_N(k_I)/dt$ being different with respect to absolute value and direction (Fig.3). An influence on the rate of change of the current control error ($d\Delta\underline{i}_N/dt$) is given here by the parameters k_I, U_z, $\underline{u}_N$, L, $\underline{i}_N$ and ω_N. As can be easily estimated, for practical applications the inductive voltage drop $L\, d\underline{i}_N/dt$ can be neglected in comparison to $\underline{u}_N$ in many cases (see Fig.3: $\Delta\varphi \to 0$).

Under stationary operating conditions one can assume sinusoidal quantities forming $\underline{u}_N$ and $\underline{i}_N$:

$$\underline{u}_N = U_N\, e^{j\omega_N t}$$
$$\underline{i}_N^* = I_N^*\, e^{j(\omega_N t + \Psi)} \qquad (5)$$

If we insert Eqs.(5)into Eq.(3) there follows ($\omega_N t = \varphi_N$):

$$L\,\frac{d\Delta\underline{i}_N}{dt} = \underline{u}_U(k_I) - e^{j\omega_N t}\,(U_N - j\omega_N L\, I_N^*\, e^{j\Psi}) \qquad (6)$$

Thereby the space vector of the current control error $\Delta\underline{i}_N$ due to Eq.(2) is represented in a coordinate system whose origin lies in the tip of $\underline{i}_N^*$. The trajectories of $\Delta\underline{i}_N(k_I)$ are trochoids which degenerate to circles for k_I=0 or k_I=7 (Fig.4). In the limiting but more theoretical case for $|\underline{u}_N| = |\underline{u}_{Ui}|$ the trajectories (for k_I=1..6) become cycloids.

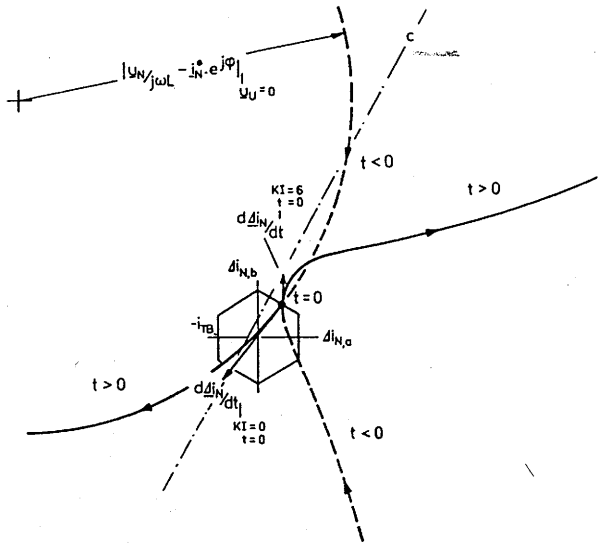

Fig.4 Trajectories of the current control error $\Delta\underline{i}_N$ shown for $|\underline{u}_U|$ close to $|\underline{u}_N|$. The "axis" C is parallel to $\underline{u}_U(k_I)$ for $k_I \neq 0,7$. For i_{TB} and the hexagon see section 3.

The rms value of $\Delta i_{N\,R,S,T}$ which is used to compare the different current controllers can be calculated from the space vector $\Delta\underline{i}_N$. At First we define:

$$\sum\Delta i^2 = \Delta i_{N_R}^2 + \Delta i_{N_S}^2 + \Delta i_{N_T}^2 \qquad (7)$$

Equation (7) characterizes the power dissipation of the system due to current control errors and can also be expressed by the space vector $\Delta\underline{i}_N$:

$$\sum\Delta i^2 = \frac{3}{2}\,|\Delta\underline{i}_N|^2 \qquad (8)$$

Accordingly,

$$\Delta i_{N_{eff}} = \sqrt{\frac{1}{T}\int_0^T \frac{1}{2}\,|\Delta\underline{i}_N|^2 dt} \qquad (9)$$

is used as a quality criterion. For converter switching frequencies in the kilohertz range for rms value calculations the trajectories of $\Delta\underline{i}_N$ can be replaced by straight lines with very good approximation (the error lies in the 0.1 per cent range).

Because, as mentioned before, for the simple hysteresis controller the maximum control error is larger than the deadband (exactly twice the deadband) a (time-) statistics is established considering the magnitude of the current control error for judging the frequency (probability) of leaving the deadband. Thereby the sum of such time intervals where $|\Delta\underline{i}_N|$ lies within the interval [I, I+ ΔI] is related to the entire time and devided by the interval width ΔI. This quotient p(I) represents (in a statistical sense) the distribution density of the absolute value of $\Delta\underline{i}_N$. From this function one can also draw conclusions with respect to the oc-

curring rms value $i_{N\,eff}$ because p(I) weighs the square of the magnitude of the state vector $\underline{i}_N$. The probability of the occurrence of a magnitude I<I' thereby follows as:

$$W(I') = \int_0^{I'} p(I)\, dI \qquad (10)$$

Remark: The current control errors represent stochastic signals in a sense of signal theory. Therefore one can only give a continous power density spectrum for them which could be obtained by a Fourier transform of the autocorrelation function. However, in this paper the analysis in the frequency domain is not persued further.

To arrive at a conclusion concerning the maximum and minimum switching frequencies of the converter legs within a fundamental period one could divide this period into equal time intervals. Then the "local" switching frequencies in these intervals would be determined. (Then one could follow an algorithm similar to the procedure for determination of the distribution density of $|\Delta\underline{i}_N|$).

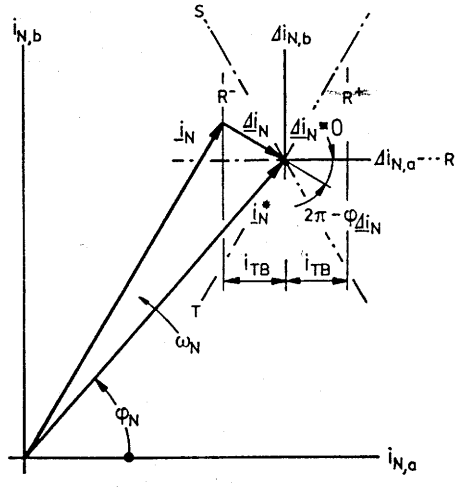

Fig.5 Current space vectors and control error stripe for phase R.

Besides the mathematical advantages of the space vector representation a very clear description of the system behavior is made possible. E.g., the deadbands around the phase current reference values are transformed into stripes lying perpendicular to the respective phase axis (see Fig.5, there shown for phase R). The common area of these stripes (i.e., the control errors of all three phases are smaller than the deadband width) results in a hexagon being characteristic for three phase on-off controllers (see Fig.7). The tip of the reference value space vector lies in the center of the hexagon. Basically one could define arbitrary areas instead of the hexagon if the control concept is based on a space vector representation of the control error (e.g., such as in [2]). Contrary to such areas only the hexagon guarantees the full use of the allowable phase current control error. The corners of the hexagon represent the simultaneous reaching of the deadband limits (one upper and one lower limit) in two phases. If one defines, e.g., the "inner circle" of the hexagon (the circle touching all six sides of the hexagon) as control error area, there results the same maximum value of the phase currents; however the smaller area leads to a higher switching frequency of the system.

3. HYSTERESIS CURRENT CONTROLLER

For this simplest form of on-off current control the converter switching status is given by three independent phase current controllers (Fig.6). Therefore, a maximum control error results being twice the deadband width. This is because the switching action of the phase where the deadband is left can only result in re-entering the deadband if the switching status of the other two phases does make this possible. (This is obviously caused by the three phase structure of the system.)

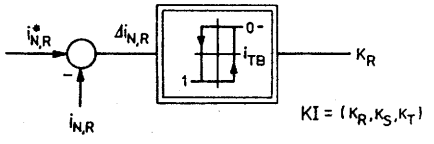

Fig.6 Hysteresis current controller (shown for phase R)

One interesting detail should be mentioned: due to the hysteresis the switching status of any phase is uniquely determined only for $\Delta i_{N\,R,S,T} > +i_{TB}$ (posive thresholds R+, S+, T+) or $< -i_{TB}$ (negative thresholds R-,S-,T-), respectively; then it is not dependent on switching history. Therefore, for a given converter switching status, e.g., (111), $\Delta\underline{i}_N$ can lie arbitrarily within the relevant region shown by Fig.7 (sectors 0,2,4,6). It follows that one can only draw limited conclusions with respect to the control error based on the switching status. On the other hand, the control error $\Delta\underline{i}_N$ determines the converter switching status definitely for the sectors 8,10,12, 14,16,18 [see, e.g. (001), sector 10].

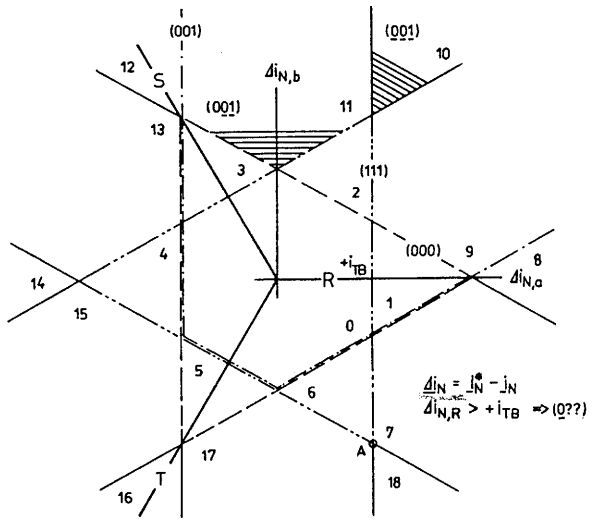

Fig.7 Tolerance area for space vector representation of $\Delta\underline{i}_N$

When the control error exceeds twice the deadband in one phase (e.g., point A in Fig.7), a switching action is enforced in the other two phases via $i_{NR}+i_{NS}+i_{NT} = 0$. Then the control error can be corrected if the DC link voltage is sufficiently large with respect to the mains voltage. (This obviously is a basic condition for the controllability of the system.) An unbiased comparison of the hysteresis controller with other on-off controllers therefore has to consider the maximum control error reached; the comparison cannot be simply based on equal deadband widths because the implicitely tolerated larger control error results in a lower switching frequency than for exact observance of the deadband. It is meaningful, however, to compare the switching frequencies, e.g., for equal rms value of the control error.

The investigation of the parameter dependency of the hysteresis controller shows that for low frequency of the AC side (assuming frequency proportional voltage amplitude, i.e. approximately constant (rated) flux in an AC machine) there occurs a significant increase of the switching frequency f_s. This frequency has as its maximum (for theoretically $|\underline{u}_N| = 0$) the value $f_s = U_z / (9.L.i_{TB})$ given for the limit cycle according to Figs.8. For decreasing AC voltage amplitude an increasing degree of a 60° symmetry is reached for the $d(\Delta\underline{i}_N)/dt$ as given for $k_T = 1...6$. This is a condition for stable switching cycles for which always neighbouring converter voltage space vectors follow each other. This is

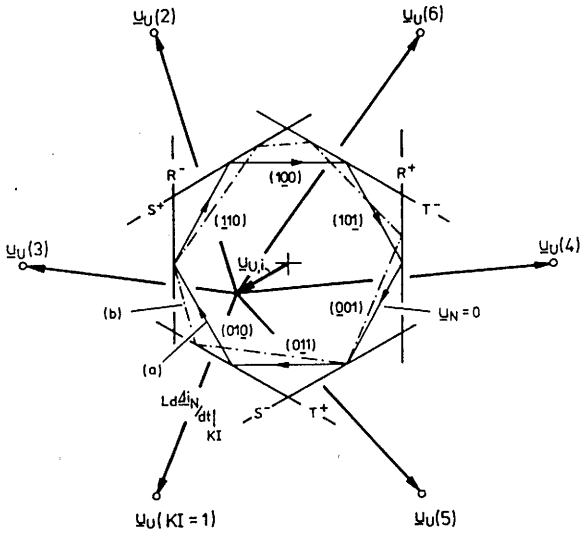

Fig.8a Limit cycles of $\Delta\underline{i}_N$ for:
a) $\underline{u}_{Ui} = 0$
b) $|\underline{u}_{Ui}| << |\underline{u}_U(k_T)|$, $k_T \neq 0,7$

because leaving the deadband results only in changing the switching state of one phase; then at most two phases can assume the same switching state because of the anti-cyclic series of switching thresholds (e.g., R+, S-,

T+, R-, S+, T-). The freewheeling state [(000) or (111) with $\underline{u}_U=0$], being most "economical" with respect to f_s is not assumed any more. The switching frequency due to the high magnitudes of the $d(\Delta\underline{i}_N)/dt$ (missing counter emf !) lies substantially above that which is obtained for higher AC voltage values. The decrease of f_s can be explained by the increasing disturbance of the symmetry of the $[d(\Delta\underline{i}_N)/dt]k_T$. As can be seen from a more detailed investigation, the existence of local temporary switching cycles with relatively high switching frequencies is also possible for higher amplitudes of $\underline{u}_N$. This effect leads to a non-monotonous function of the switching frequency versus the mains voltage (frequency). The switching frequency behavior shown to be smooth in Figs.12,13 therefore only is a good approximation of the real situation.

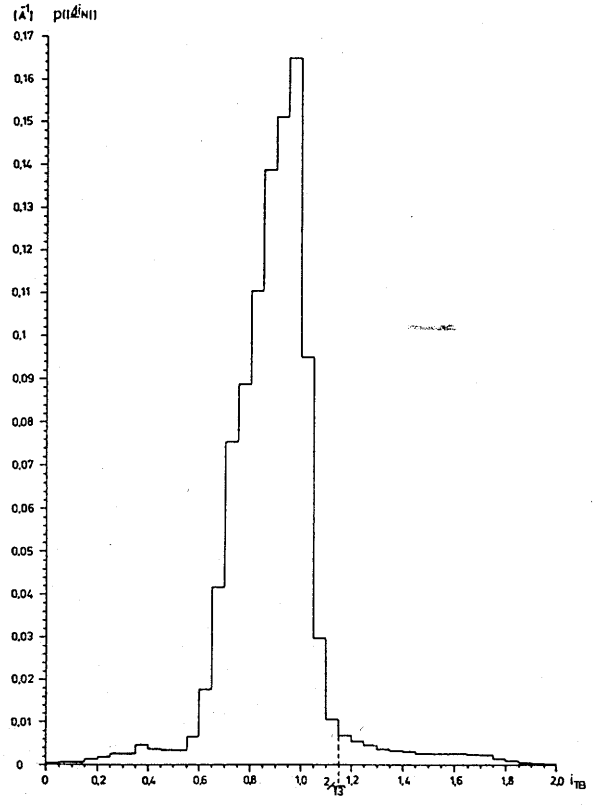

Fig.8b Distribution density of $|\Delta\underline{i}_N|$; (f_N=5 Hz, U_{Neff}=22 V, $|\underline{i}_N^*|$ = 25 A, U_z = 620 V, i_{TB} = 2 A, L=6.2 mH). Due to the limit cycle (Fig.8a) $\Delta\underline{i}_N$ moves close to the border of the tolerance area.

A further operating condition, being characteristic for the hysteresis controller, exists in the region $|\underline{u}_U|/|\underline{u}_N| \approx 2$: the control error of one phase can be kept within its deadband for an interval of about 60° of the AC voltage without any switching action of the respective phase. This can be explained by the $d(\Delta\underline{i}_N)/dt$ (Fig.9) of the converter output voltage space vectors being approximately symmetric with reference to $\underline{u}_{Ui}$; these vectors are chosen in a cyclic manner [e.g. (001)-(101)-(100)-(000) or (100)-(101)-(001)-(000)]. The cycle is stable due to the switching conditions (thresholds of phases R and T); the stability is interrupted only by turning of the $\underline{u}_N$ space vector. The phase not involved in the switching cycle above mentioned (Phase S in Fig.9) is given by

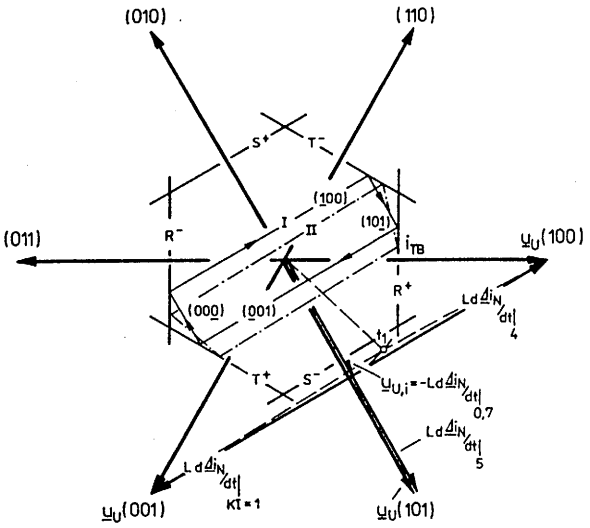

Fig.9 I. switching cycle for $\underline{u}_N \perp$ S-II. angle change of $\underline{u}_N$ (at time t_1) results in a disturbance of the symmetry given for I.

the direction of the mains voltage vector. Via the (average) antiparallelism of the two vectors of approximately equal magnitude $[d(\Delta\underline{i}_N)/dt]_0$, $[d(\Delta\underline{i}_N)/dt]_1$ the cycle is kept so to say in "equilibrium" between S+ and S-. After a medium angle change of the voltage vector $\underline{u}_N$ by about 60° the cycle tips over also by 60° and then occurs between the thresholds of S and T in the case considered here.

Then R is not involved in the switching cycle. The occurrence of the effect described is made possible only by the fact that the DC link center point has a free potential versus the AC voltage neutral; therefore the switching actions in one phase influences the current behavior in the other two phases.

The AC voltage fundamental produced by the converter has to balance the mains voltage (including the inductive voltage drop $\underline{i}_N \cdot \omega_N \cdot L$) for current control according to the given reference values. The differences between this ideal converter voltage $\underline{u}_{Ui}$ and the actual output space vectors $\underline{u}_U(k_I)$ of constant magnitude determine the time derivative of the current control error. Thereby the $\underline{u}_U(k_I)$ being closest (with regard to magnitude and phase) to the mains voltage show the smallest value of current change. Based on these conditions the switching frequency decreases with increasing AC voltage amplitude and/or with decreasing voltage margin of the converter. With a deadband control the reference value in the average is only reached for a sufficiently high switching number within the AC voltage period. For the case of a small difference between mains and converter voltage this condition is not met any more; the reference value is assumed in the average only for more than one AC voltage period. This leads to subharmonics which result in the case of a drive system in higher AC machine losses. If the voltage margin becomes 0, the voltage equilibrium mentioned can not be maintained any more; the system looses controllability and the maximum control error becomes larger than $2.i_{TB}$. This problem could be always handled by an accordingly high DC link voltage U_z; however, this problem remains in practical applications due to the economically required voltage utilization of the switching devices and/or due to a technologically given limit of U_z.

In the following the dependency of the hysteresis controller switching frequency on the essential system parameters shall be shown. Because the measured distribution density of $|\Delta\underline{i}_N|$ (Fig.10) shows a geometrically similar behavior at

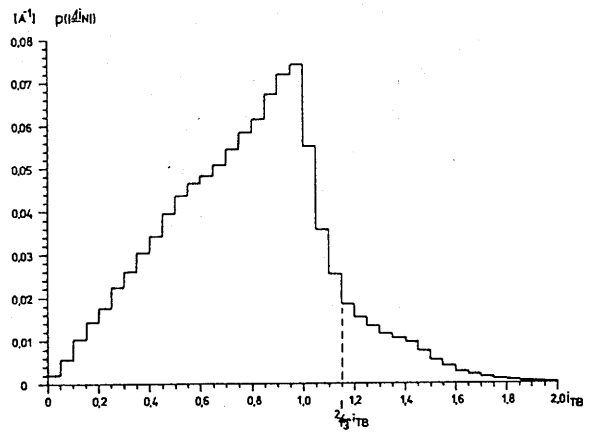

Fig.10 Hysteresis controller: Distribution density of $|\Delta\underline{i}_N|$; (f_N = 50 Hz, U_{Neff} = 220 V, $|\underline{i}_N^*|$=25 A, U_z=620 V, i_{TB}=2 A, L=6.2 mH). $2/\sqrt{3}\ i_{TB}$: radius of the "outer circle" of the tolerance area.

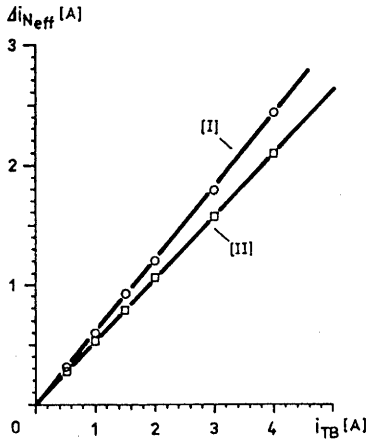

Fig.11 RMS value of the control error as a function of i_{TB} (half the deadband width); (f_N=50 Hz, U_{Neff}=220 V, $|\underline{i}_N^*|$ = 25 A, U_z = 620 V, i_{TB}=2 A, L=6.2 mH).
I. hysteresis controller:
$\Delta i_{Neff}/i_{TB} \approx 0.61$
II. predictive controller:
$\Delta i_{Neff}/i_{TB} \approx 0.52$
For equal i_{TB} we have: $\Delta i_{Neff}(I) > \Delta i_{Neff}(II)$ because for the predictive controller $\Delta\underline{i}_N$ is controlled inside the hexagon in any case (however, this is connected with higher f_s).

different DC link voltages (constant AC voltage), we can give an (approximately) constant relationship between deadband width and rms value of the control error (Fig.11). As shown in Fig.12 the product of inductance and switching frequency is about constant, the switching frequency decrease is approximately proportional to 1/L. For variable DC link voltages the relationship of the switching frequencies corresponds to the voltage margin of the converter. From $L.d(\Delta\underline{i}_N)/dt \approx \underline{u}_U - \underline{u}_N$ there follows that the product $i_{TB}.f_s$ is constant (Fig.13) for fixed values of $|\underline{u}_U|$, $|\underline{u}_N|$ and L. Also here the same is valid for the switching frequencies occurring for different DC link voltages as said for Fig.13.

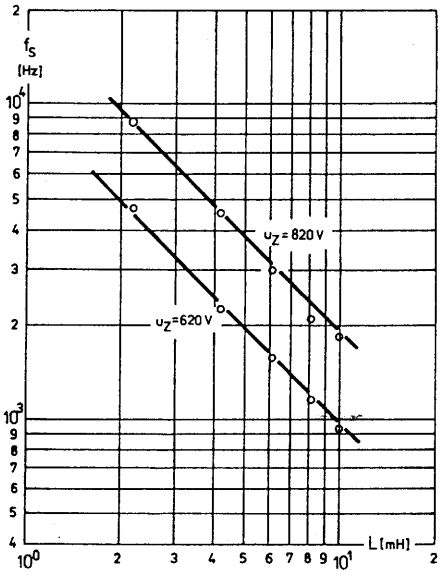

Fig.12 Hysteresis controller: Switching frequency as a function of the inductance. (f_N = 50 Hz, U_{Neff} = 220 V, $|\underline{i}_N^*|$=25 A, U_Z=620 V, i_{TB} = 2 A). The deviation of the linear behavior (applying logarithmic scales) for higher values of L can be explained by the then given stronger curvature of the trajectories. $f_s.L$= constant is only valid if the trajectories can be approximated by straight lines. Moreover $f_s.L$ = constant neglects all "resonance" - effects (see Fig. 24) of f_s.

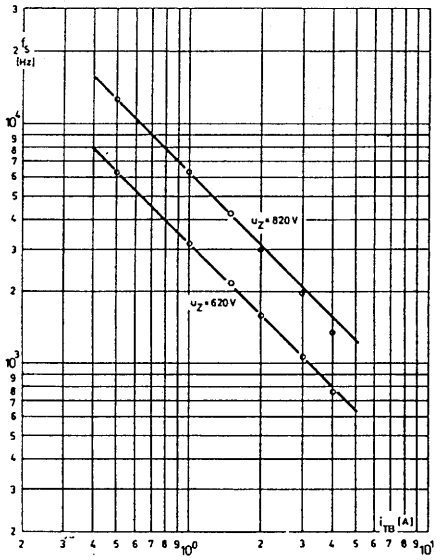

Fig.13 Hysteresis controller: Switching frequency as a function of i_{TB} (half deadband width); (f_N = 50 Hz, U_{Neff} = 220 V, $|\underline{i}_N^*|$=25 A, U_Z=620 V, L=6.2 mH).

4. PREDICTIVE CONTROLLER

As described in section 3 the control error can assume a maximum value of twice the deadband width in the case of simple hysteresis control. This is due to the indepenent phase current controllers. If $\Delta\underline{i}_N$ has to be controlled such that it remains within the i_{TB}-tolerance region (hexagon), the reaction of the whole system to a switching decision has to be considered before it is "executed" by the converter. Certainly excluded should be that (old) switching state k which actually makes necessary a converter switching status change (because the relevant trajectory leaves the hexagon). In general more than one of the remaining seven (only six for k=0 or k=7) possible switching states will guide back the control error into the hexagon (Fig.14). Among these a selection has to be made in an optimal sense.

One possible optimization criterion is, e.g., the maximization of the dwell time [$t(k_I)$] of the trajectory within the hexagon, weighed by

the number of necessary switchings $n(k,k_x)$ to get from the old converter switching status k to the new one k_x (Fig.15). This acts as a switching frequency minimization. But via $n(k,k_x)/t(k_x)$ only the local switching frequency is minimized (as, e.g., in a steepest descent method) and does not necessarily mean that the global minimum will be found (compare I in Fig.15). On the other hand, a global optimization in practice cannot be performed due to the enormous computational effort connected herewith.

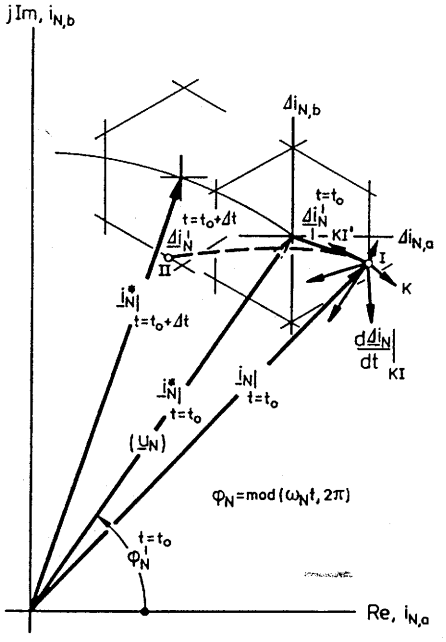

Fig.14 Operation of the predictive controller: For $t=t_o$ $\Delta\underline{i}_N$ reaches the tolerance area limit in I. The changing of the converter switching status from k to k_x leads $\Delta\underline{i}_N$ back into the hexagon; then $\Delta\underline{i}_N$ does not leave it until $\Delta t=t(k_x)$ in II.

An other optimization criterion could be, e.g., to minimize the (local) contribution of the considered part of the trajectory to the rms value of the control error. Also in this case the optimization criterion can be mathematically formulated easily.

The control of $\Delta\underline{i}_N$ within the tolerance area (which is the "constraint" of the optimization) can only be guaranteed if at least one of the $[d(\Delta\underline{i}_N)/dt]k_x$ leads back into the hexagon. From this the controllability margin (being in general dependent on the geometrical form of the tolerance area) of the predictive controller can be derived (Fig.16). The optimization of course is only

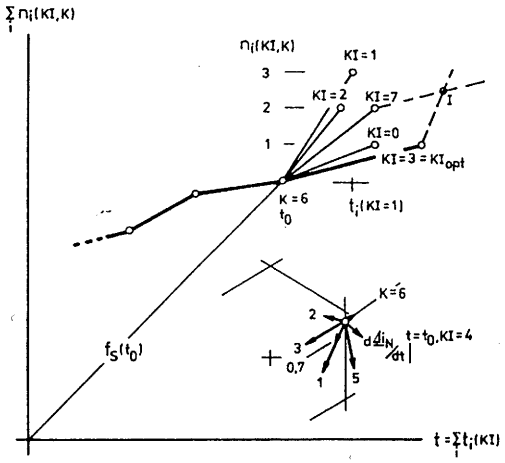

Fig.15 Predictive controller: Minimization of f_s; $t(k_x)$ weighed by $n(k,k_x)$ correspond to the reciprocal value of the "local" switching frequency in $t=t_o$. The "global" switching frequency $f_s(t_o)$ is determined by $\Sigma[n(k,k_x)] / \Sigma t_i(k_x)$.

possible if at least two k_x exist fulfilling the constraint. As the analysis of the switching decisions chosen by the optimization procedure shows, for $|\underline{u}_N|$ close to $|\underline{u}_U|$ - relatively independent of the weighing by $n(k,k_x)$ - frequently such switching states are selected where the converter output voltage vector is close to the mains voltage; this results in a correspondingly low magnitude of the $d(\Delta\underline{i}_N)/dt$. In the case of $|\underline{u}_N| << |\underline{u}_U|$ the $[d(\Delta\underline{i}_N)/dt]k_x$ show about equal magnitudes (with exeption of the freewheeling state which is taken on in a preferred manner). The selection of the switching decision (besides k_x = 0,7) then is essentially influenced by the $n(k,k_x)$.

The investigation in this sec-

tion is limited to the stationary operating behavior of the predictive controller. In a dynamic sense its function is limited by the converter voltage margin. This is because with Eq.(3) for high $d(\underline{i}_N^*)/dt$ the value of $d(\Delta\underline{i}_N)/dt$ is mainly determined by the reference value. To handle this operating condition a further control concept (e.g., a hysteresis controller) is to be superimposed onto the predictive controller; this controller brings the transient (possibly large) control error back into the tolerance region.

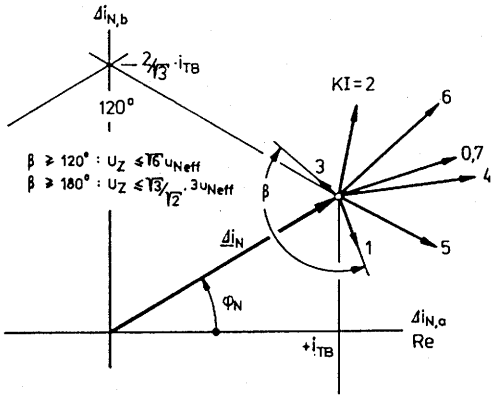

Fig.16 Predictive controller controllability margin: For $\beta > 120°$ possibly (dependent on $\underline{u}_N$) no trajectory guides $\Delta\underline{i}_N$ back into the hexagon from one of it`s corners. If $\Delta\underline{i}_N$ lies on the edges of the hexagon $\beta < 180°$ is sufficient that there is at least one trajectory leading back into the hexagon.

For the dependencies of the characteristic quantities on the system parameters (Figs. 11, 17, 18, 19) essentially the same is valid as said for the hysteresis controller. The characteristic of the switching frequency as a function of the mains voltage amplitude can be explained as follows: for small AC voltages the freewheeling state is taken due to the optimization in a preferred manner (Fig.24); this is opposed to the hysteresis controller. The system remains in the freewheeling state for a longer period of time due to the small $[d(\Delta\underline{i}_N)/dt]_{0,7}$; this results in a low switching frequency. If $|\underline{u}_N|$ lies close to $|\underline{u}_U|$ there again switching states occur (close to the mains voltage vector) showing a low $d(\Delta\underline{i}_N)/dt$; this results in a decrease of the switching frequency f_s for higher AC voltages. For $|\underline{u}_U| \approx 2.|\underline{u}_N|$ "resonant cycles" similar as in the case of the hysteresis controller can be observed, despite the optimization performed. These cycles result in an increased f_s, which can be explained by the then given high degree of symmetry of the $[d(\Delta\underline{i}_N)/dt]k_I$. The switching frequency trend again can only be described as approximately smooth.

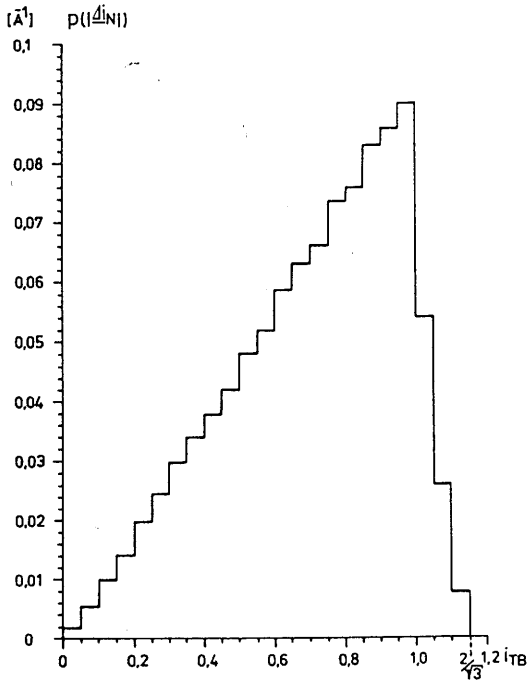

Fig.17 Predictive controller: Distribution density of $|\Delta\underline{i}_N|$; (f_N = 50 Hz, U_{Neff} = 220 V, $|\underline{i}_N^*|$ = 25 A, U_Z = 620 V, L= 6.2 mH, i_{TB} = 2 A). $2/\sqrt{3}\ i_{TB}$ is the radius of the "outer circle" of the tolerance area. Because the tolerance area is not left (due to the constraint of the optimization) $p(|\Delta\underline{i}_N|) = 0$ is valid for $|\Delta\underline{i}_N| > 2/\sqrt{3}\ i_{TB}$.

5. OFF-LINE OPTIMIZED PREDICTIVE CONTOLLER - CONTROL TABLE

As mentioned in section 4, the

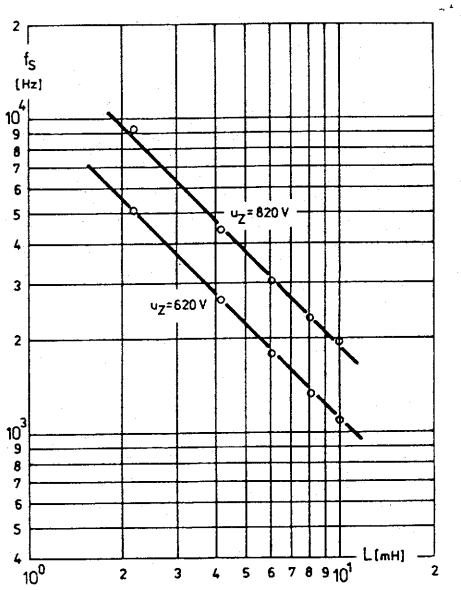

Fig.18 Predictive controller: Switching frequency as a function of inductance; (f_N= 50 Hz, U_{Neff}=220 V, $|\underline{i}_N^*|$=25 A, U_Z=620 V, i_{TB}=2 A). Due to $|\Delta\underline{i}_N| < i_{TB}$, f_S lies above that of the hysteresis controller with equal parameters.

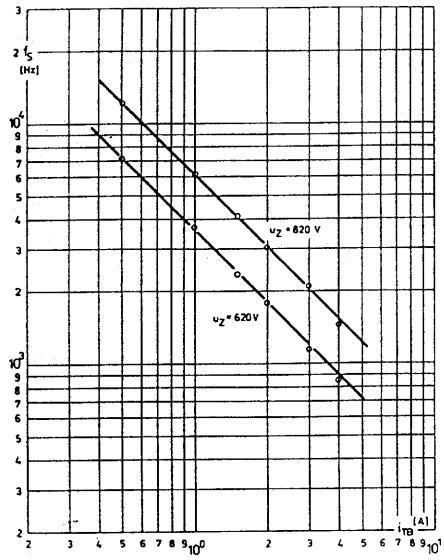

Fig.19 Predictive controller: switching frequency as a function of i_{TB} (half deadband width); (f_N = 50 Hz, U_{Neff}= 220 V, $|\underline{i}_N^*|$=25 A, U_Z=620 V, L = 6.2mH).

predictive controller requires knowledge about the instantaneous system state k to select the optimal new switching state k_I. In the stationary case considered here the system state is characterized by $\underline{u}_N$, $\underline{i}_N$, $\Delta\underline{i}_N$ and the switching state k existing until now. According to Eq.(6) $\underline{i}_N$ exerts only very small influence on the $[d(\Delta\underline{i}_N)/dt]k_I$ (and consequently on f_S, Fig.20) for small values of L (as mostly given in real systems), because then $|\underline{u}_N| >> \omega_N.L.|\underline{i}_N^*|$. The inductive voltage drop essentially causes only a rotation of $\underline{u}_N$ by an angle of a few degrees. This is of little significance because $\underline{u}_U$ can assume only six different directions with an angle of 60° between them. Therefore the switching decision of the predictive controller is almost independent of the magnitude I_N of $\underline{i}_N$ and primarily determined by $\underline{u}_N$, $\Delta\underline{i}_N$ and k.

For a given value of the mains voltage therefore the optimal k_I can be given by eight tables for the different k if a sufficiently fine discretization of $\varphi\underline{u}_N$ and $\varphi\Delta\underline{i}_N$ (arguments of $\underline{u}_N$ and $\Delta\underline{i}_N$) is made (6° in Fig.21). For a given output state k only such new states (k_I) are listed for which the trajectory corresponding to k would cross the tolerance region boundary (hexagon) from the inside. Only those values are needed if $\Delta\underline{i}_N$ is controlled within the hexagon (which is guaranteed by the working principle of the predictive controller). The other locations in the table (indicated by "8" in Fig.21) could be filled, e.g., by k_I=k because k there leads (already) back into the hexagon without making switching necessary.

As shown in Fig.21, different k_I appear (with good approximation) only in 30°-segments of the table. This can be explained basically by the 30° symmetry of the tolerance region in connection with the 60° discrete directions of $\underline{u}_U$. The expectation being obvious therefore, namely that the predictive controller can be described by switching tables of relatively less extent (Fig.22), is proven by simulation. The high effort connected with the on-line optimizing predictive controller [2] can be avoided by an off-line optimization

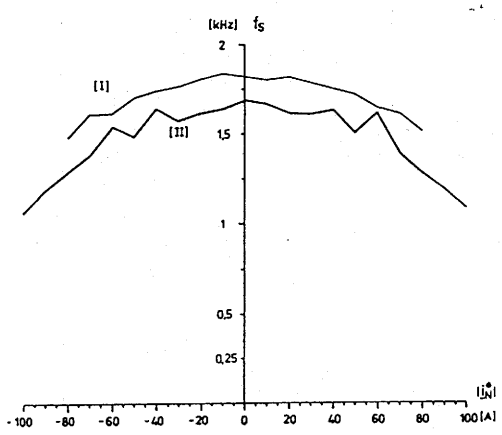

Fig.20 Switching frequency as a function of the current reference value $|\underline{i}_N^*|$; (f_N = 50 Hz, U_{Neff} = 220 V, U_Z = 620 V, i_{TB} = 2 A, L=6.2mH). $|\underline{i}_N^*| < 0$ stands for ϕ =180° (power conversion from the DC to the AC side).
I. predictive controller
II. hysteresis controller
("measuring points": every multiple of 10 A, linear interpolation); f_s decreases with increasing $|\underline{i}_N^*|$; this can be explained by the then higher counter voltage $\underline{u}_{Ui}$ (increased voltage across L).

	0	30	60	90	120	150	180	210	240	270	300	330
336	88888	88888	88888	88888	88888	88888	88888	88888	88888	88888	88888	88888
342	88888	88888	88888	88888	88888	88888	88888	88888	88888	88888	88888	88888
348	88888	88888	88888	88888	88888	88888	88888	88888	88888	88888	88888	88888
354	88888	88888	88888	88888	88888	88888	88888	88888	88888	88888	88888	88888
0	88888	88888	88888	88888	88888	88888	88888	88888	88888	88888	88888	88888
6	88888	88888	88888	88888	88888	88888	88888	88888	88888	88888	88888	88888
12	88888	88888	88888	88888	88888	88888	88888	88888	88888	88888	88888	88888
18	88888	88888	88888	88888	88888	88888	88888	88888	88888	88888	88888	88888
24	88888	88888	88888	88888	88888	88888	88888	88888	88888	88888	88888	88888
30	30000	00000	00000	00000	03333	33333	33333	33333	33333	33333	33333	33333
36	30000	00000	00000	00000	00000	00003	33333	33333	33333	33333	33333	33333
42	30000	00000	00000	00000	00000	00000	03333	33333	33333	33333	33333	33333
48	30000	00000	00000	00000	00000	00000	03333	33333	33333	33333	33333	33333
54	30000	00000	00000	00000	00000	00000	03333	33333	33333	33311	11111	11133
60	10000	00000	00000	00000	00000	00000	03333	33311	11111	11111	11111	11111
66	10000	00000	00000	00000	00000	00000	01111	11111	11111	11111	11111	11111
72	10000	00000	00000	00000	00000	00000	01111	11111	11111	11111	11111	11111
78	10000	00000	00000	00000	00000	00000	01111	11111	11111	11111	11111	11111
84	10000	00000	00000	00000	00000	00000	01111	11111	11111	11111	11111	11111
90	11111	11111	10000	00000	00000	00000	01111	11111	11111	11111	11111	11111
96	11111	11111	10000	00000	00000	00000	00000	00000	01111	11111	11111	11111
102	55555	55511	10000	00000	00000	00000	00000	00000	01111	11111	11111	15555
108	55555	55555	50000	00000	00000	00000	00000	00000	01111	11115	55555	55555
114	55555	55555	50000	00000	00000	00000	00000	00000	01555	55555	55555	55555
120	55555	55555	50000	00000	00000	00000	00000	00000	05555	55555	55555	55555
126	55555	55555	40000	00000	00000	00000	00000	00000	05555	55555	55555	55555
132	55544	44444	40000	00000	00000	00000	00000	00000	05555	55555	55555	55555
138	44444	44444	40000	00000	00000	00000	00000	00000	04445	55555	55555	44444
144	44444	44444	40000	00000	00000	00000	00000	00000	04444	44444	44444	44444
150	44444	44444	44444	44444	40000	00000	00000	00000	04444	44444	44444	44444
156	44444	44444	44444	44444	40000	00000	00000	00000	00000	00000	04444	44444
162	44444	44444	44444	44444	40000	00000	00000	00000	00000	00000	04444	44444
168	44444	44444	44444	44444	40000	00000	00000	00000	00000	00000	04444	44444
174	44444	44444	44444	44444	40000	00000	00000	00000	00000	00000	04444	44444
180	44444	44444	44446	66666	60000	00000	00000	00000	00000	00000	04444	44444
186	44444	66666	66666	66666	60000	00000	00000	00000	00000	00000	06664	44444
192	66666	66666	66666	66666	60000	00000	00000	00000	00000	00000	06666	66666
198	66666	66666	66666	66666	60000	00000	00000	00000	00000	00000	06666	66666
204	66666	66666	66666	66666	66600	00000	00000	00000	00000	00000	06666	66666
210	66666	66666	66666	66666	66666	66666	60000	00000	00000	00000	06666	66666
216	88888	88888	88888	88888	88888	88888	88888	88888	88888	88888	88888	88888
222	88888	88888	88888	88888	88888	88888	88888	88888	88888	88888	88888	88888
228	88888	88888	88888	88888	88888	88888	88888	88888	88888	88888	88888	88888
234	88888	88888	88888	88888	88888	88888	88888	88888	88888	88888	88888	88888
240	88888	88888	88888	88888	88888	88888	88888	88888	88888	88888	88888	88888
246	88888	88888	88888	88888	88888	88888	88888	88888	88888	88888	88888	88888
252	88888	88888	88888	88888	88888	88888	88888	88888	88888	88888	88888	88888
258	88888	88888	88888	88888	88888	88888	88888	88888	88888	88888	88888	88888
264	88888	88888	88888	88888	88888	88888	88888	88888	88888	88888	88888	88888
270	88888	88888	88888	88888	88888	88888	88888	88888	88888	88888	88888	88888
276	88888	88888	88888	88888	88888	88888	88888	88888	88888	88888	88888	88888
282	88888	88888	88888	88888	88888	88888	88888	88888	88888	88888	88888	88888
288	88888	88888	88888	88888	88888	88888	88888	88888	88888	88888	88888	88888
294	88888	88888	88888	88888	88888	88888	88888	88888	88888	88888	88888	88888
300	88888	88888	88888	88888	88888	88888	88888	88888	88888	88888	88888	88888
306	88888	88888	88888	88888	88888	88888	88888	88888	88888	88888	88888	88888
312	88888	88888	88888	88888	88888	88888	88888	88888	88888	88888	88888	88888
318	88888	88888	88888	88888	88888	88888	88888	88888	88888	88888	88888	88888
324	88888	88888	88888	88888	88888	88888	88888	88888	88888	88888	88888	88888
330	88888	88888	88888	88888	88888	88888	88888	88888	88888	88888	88888	88888

Fig.21 Switching table of the predictive controller; horizontal: $\varphi\Delta\underline{i}_N$, vertical: $\varphi\underline{u}_N$ (both given in steps of 6°). (f_N=5 Hz, U_{Neff}=22 V, $|\underline{i}_N^*|$= 25 A, U_Z=620 V, i_{TB}=2 A, L= 6.2mH, instantanous switching state k=2). The table provides the optimal new switching state k_I.

stored in tables (for different k) with relatively small storage requirements.

The problem of making one (medium) switching decision for a whole 30°x30° segment is, besides the then not always given optimality, that the chosen k_I does not guide $\Delta\underline{i}_N$ back into the hexagon in each case. The second control concept which has to be superimposed on the predictive controller to handle transient conditions (see section 4) then also has to interact occasionaly for stationary working conditions in order to correct the control error. An exact definition of the maximum control error therefore is not possible. As an analysis of the distribution density of $|\Delta\underline{i}_N|$ shows (Fig.23), the deviation from the behavior of the on-line optimizing predictive controller is relatively small. This is because the maximum value of $\Delta\underline{i}_N$ exceeds i_{TB} only by a small amount and this also occurs very seldom. An essential influence on the rms value of $\underline{i}_N$ thereby is not given.

With a predictive controller a significant reduction of the switching frequency (compared to the hysteresis controller) is possible especially for low frequencies of the AC side (assumption: $|\underline{u}_N|/\omega_N$ = constant resulting in an approximately constant flux of an AC machine). As described before this is achieved due

to the then very small $d(\Delta \underline{i}_N)/dt$ of the freewheeling states. As the investigations show, a controller with a 30° discrete switching table (established, e.g., for f_N=5 Hz, Fig.22) may lower the switching frequency even beneath that of the on-line predictive controller (Fig.24). This phenomenon can be explained by the fact that the optimization is performed only according to the "local" switching frequency; furthermore the "resonant cycles" of the on-line predictive controller (described in section 4) cause an increase of the switching frequency as compared to its (global) minimum possible value. Moreover due to these cycles the freewheeling trajectory will be situated in a preferred manner close to the tolerance area boundaries which would increase the rms value of $\Delta \underline{i}_N$. The "disturbed" optimization given by the not exact (not "sufficiently" fine) switching table avoids such resonant cycles for the table-based controller. The investigations performed show that the table proves to be extremely robust and leads for a wide AC voltage region to switching

2	2	2	2	2	2	2	2	2	2	2	2
2	2	2	2	2	2	2	2	2	2	2	2
0	0	0	0	0	0	3	3	3	3	3	3
0	0	0	0	0	0	1	1	1	1	1	1
5	5	0	0	0	0	0	0	1	1	5	5
4	4	0	0	0	0	0	0	4	5	5	4
4	4	4	4	0	0	0	0	0	0	4	4
6	6	6	6	0	0	0	0	0	0	6	6
2	2	2	2	2	2	2	2	2	2	2	2
2	2	2	2	2	2	2	2	2	2	2	2
2	2	2	2	2	2	2	2	2	2	2	2
2	2	2	2	2	2	2	2	2	2	2	2

Fig.22 Simplified switching table derived from Fig.21; resolution of 30° for $\varphi \Delta \underline{i}_N$ (horizontal) and $\varphi \underline{u}_N$ (vertical).

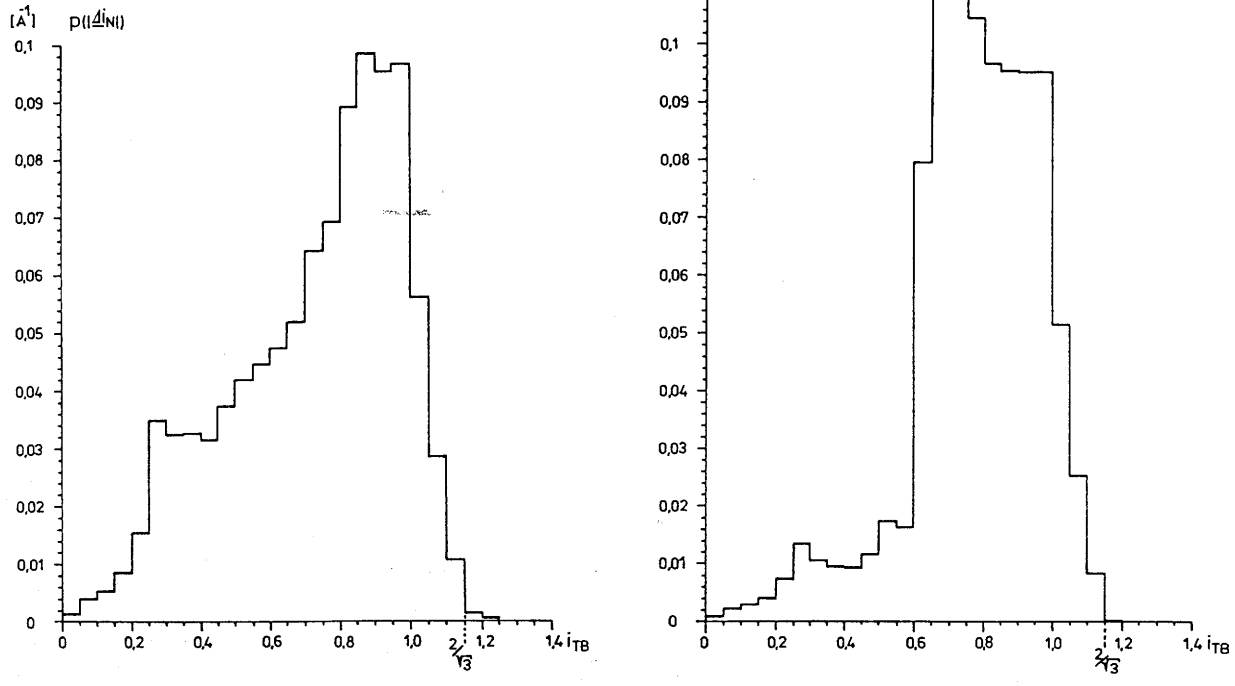

Fig.23 Distribution density of $|\Delta \underline{i}_N|$; (f_N=5 Hz, U_{Neff}=22 V, $|\underline{i}_N^*|$=25 A, U_z=620 V, i_{TB}=2 A, L=6.2mH, instantanous switching state k=2);
a) (left) : off-line optimized control table
b) (right): predictive controller
The smaller Δi_{Neff} of a) compared to b) (see Fig.24, f_N=5 Hz) is due to the "disturbed" optimization of the table based controller (avoidance of "resonant" switching cycles).

frequencies being smaller than those of the on-line predictive controller with an approximately equal rms value of $\Delta\underline{i}_N$ (Fig.24). In the vicinity of $|\underline{u}_U| \approx 2.|\underline{u}_N|$ the switching table has only limited validity (because it is based, as mentioned before, on f_N = 5 Hz). The superimposed control system (in the present case a hysteresis controller) has to interact more and more to correct the control error. The switching frequency lies, as that of the on-line predictive controller, in the region of the hysteresis controller. Basically then the effect of an optimization is not noticeable because the magnitudes of the $[d(\Delta\underline{i}_N)/dt]k_I$ are not very different. Moreover the (locally effective) optimization criterion cannot eliminate "resonant cycles" appearing due to symmetries (leading to trajectories similar to those shown in Fig.8a or 9).

In practical applications a substitution of the on-line predictive controller (avoiding the high effort connected with it) by a table based controller is possible. Then for lower AC voltages the switching decisions of this controller are taken from an off-line optimized switching table; at higher AC voltages the system is switched over to the superimposed hysteresis controller. This transition therefore can be performed quasi continously because the switching decisions for the hysteresis controller can also be put into tables easily; the "switching over" only means an exchange of the switching table. "Switching over" takes place in the case of operation based on the optimized control table too, if the optimized switching decision does not lead back the $\Delta\underline{i}_N$ into the tolerance area.

The complex plane is divided into 19 segments (sectors) by the 6 thresholds (Fig.7) which are determined by corresponding Δi_{NR}, Δi_{NS}, Δi_{NT}. With an additional evaluation of $\Delta i_{NR} - \Delta i_{NS}$, $\Delta i_{NS} - \Delta i_{NT}$ and $\Delta i_{NT} - \Delta i_{NR}$ a 30° sector for $\Delta\underline{i}_N$ (necessary for the table based controller) can be determined by a simple comparator circuit. The evaluation of the $\underline{u}_N$ is

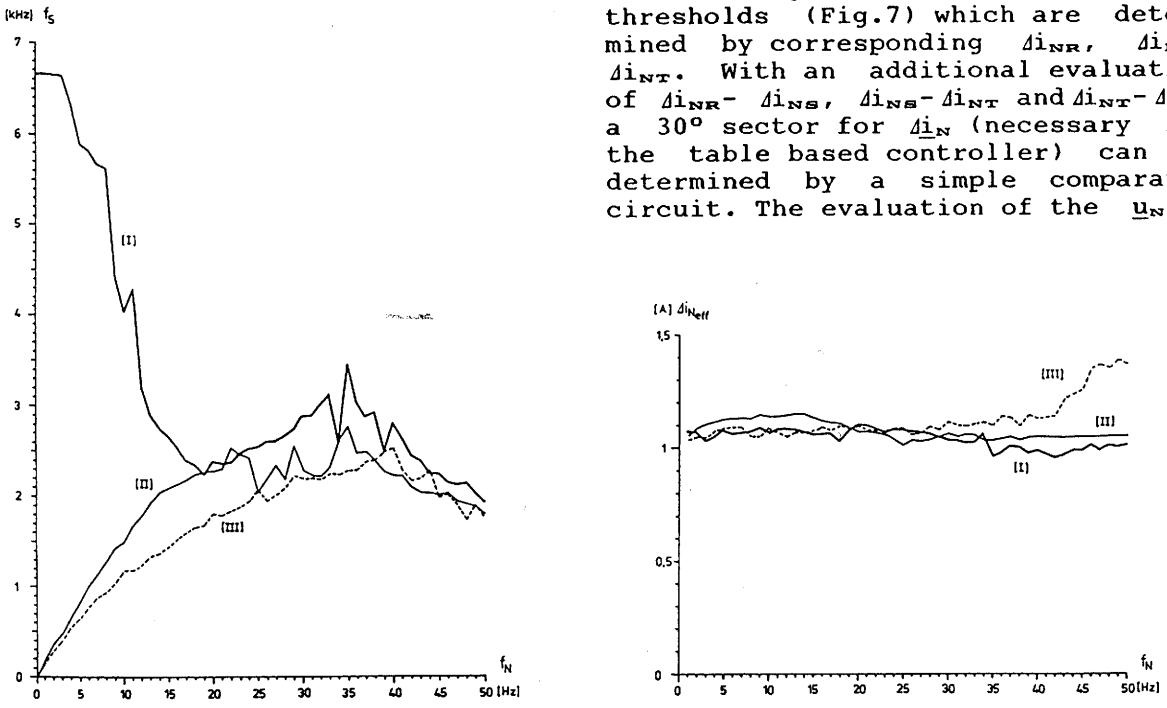

Fig.24 Comparison of switching frequencies and rms values of $\Delta\underline{i}_N$ for the control concepts treated:

I. Hysteresis controller (i_{TB} = 1.67 A)
II. Predictive controller (i_{TB} = 2 A)
III. Optimized control table (i_{TB} = 2 A), optimized for f_N = 5 Hz, U_{Neff} = 22 V

An approximately equal rms value of Δi_{Neff} is achieved with the mentioned i_{TB} values. If i_{TB} is adapted to keep Δi_{Neff} constant exactly, $f_S = f_S(f_N)$ would be smoother than shown. ($|\underline{i}_N^*|$ = 25 A, U_Z=620 V, L=6.2mH, U_{Neff}/f_N = constant = 220V/50Hz).

also performed via the phase quantities u_{NR}, u_{NS}, u_{NT}.

As mentioned before the table based operation is switched over to a pure hysteresis controller operating at higher AC voltages. This requires establishing of $|\underline{u}_N|$ by (1) in Fig.25 (e.g., a simple rectifier followed by a comparator). If the table based controller is part of a drive control system the AC voltage ("mains") is realized by the inner (counter) emf of the motor; this voltage therefore is not accessible directly but often calculated anyhow to control the flux of the motor. If this is done by digital control (1) and (2) of Fig.25 can be omitted.

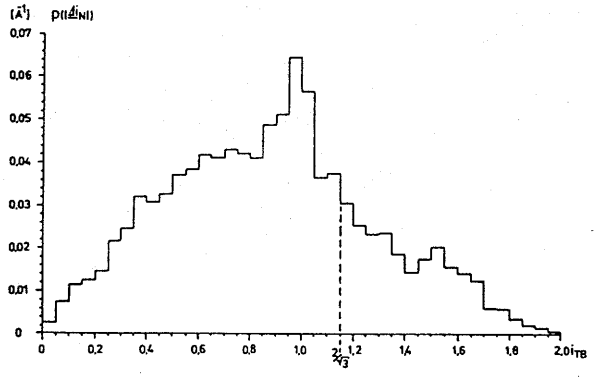

Fig.24a Table-based controller (optimization for f_N = 5 Hz, U_{Neff} = 22 V): Distribution density of $|\Delta\underline{i}_N|$; (f_N = 50 Hz !, U_{Neff} = 220 V, $|\underline{i}^*_N|$ = 25 A, U_Z = 620 V, i_{TB} = 2A, L = 6.2mH).

The table based controller shown in Fig.25 basically represents a synchronous state sequencer. This requires a clock-synchronous transfer of the input variables. To detect the crossed threshold the sector number s_i (supplied by $\Delta\underline{i}_N$ comparators I and II) is compared with s_{i-1} (the sector number delayed by one clock cycle) by the $\Delta\underline{i}_N$ encoder (8). It is assumed that the clock frequency is sufficiently high that within one clock cycle only transfers between directly neighbouring sectors are possible. Then this information can be expressed as a 6-bit data word if the information for the predictive con-

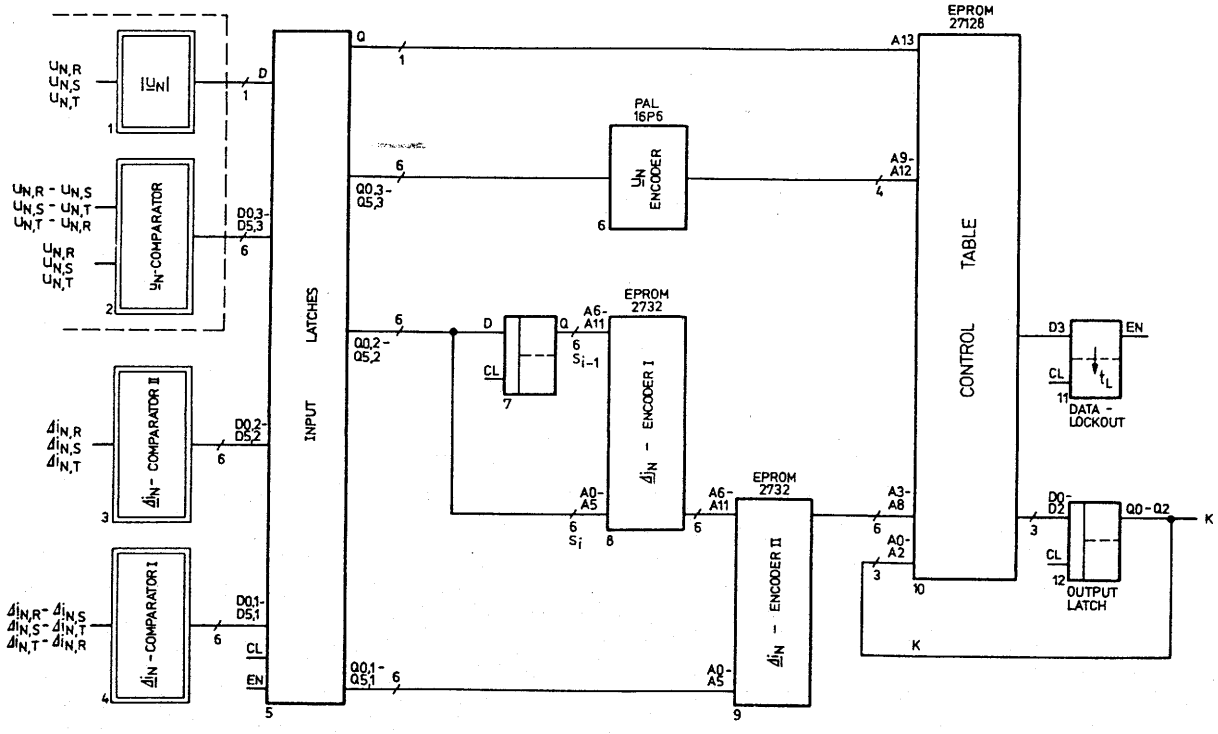

Fig.25 Realization of the off-line optimized (table-based) predictive controller as a synchronous state sequencer.

troller is included. The $\Delta\underline{i}_N$ comparator I (4) forms a tolerance region which is tilted by 30° compared to that region determined by (3) (Fig.26). (From this there follows the possibility to evaluate $\varphi\Delta\underline{i}_N$ in 30° segments.) The $\Delta\underline{i}_N$ encoder II (realized as 32k-bit EPROM such as encoder I) transfers the information concerning $\Delta\underline{i}_N$ to the control table if the system trajectory moves from the hexagon into a neighbouring sector (this means that a "predictive controller decision" has to be made). If the control error cannot be turned back by that, boundaries of outer sectors will be crossed. The information that hysteresis controller operation has to be selected in this case is also contained in the encoder II (9) output (6-bit). The pure hysteresis controller operation for higher AC voltages is selected by (1).

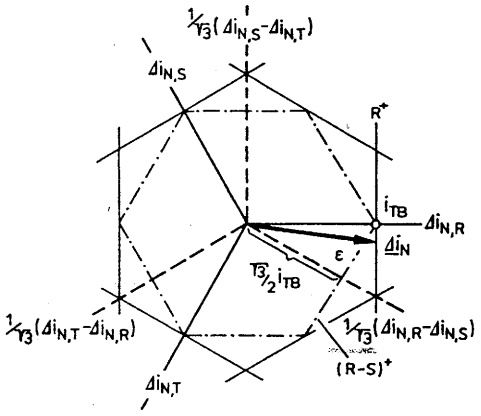

Fig.26 Superposition of two tolerance areas (I and II) tilted 30° with respect to each other for receiving a 30° resolution for $\varphi\Delta\underline{i}_N$; for the case shown here the position of $\Delta\underline{i}_N$ can be clearly related to the corresponding 30° sector given by R+ and (R-S)+ = 1.

The output of a new switching state is delayed by one clock cycle such that the previous switching state (required for predictive controller decisions) is available to the control table. Due to the realization as a sychronous state sequencer a change of the system variables is recognized within one clock cycle. It leads to the output of a new switching state and activates the data-lockout circuit (11). The data-lockout (realized as a clock-synchronous monostable multivibrator) temporarily inhibits the update of the system state variables (5). This is required because the controlled system responds to the new switching state (output by the controller) only after the converter delay time. A change of the control output during this time is not meaningful. The converter delay time therefore is the minimum value for the data-lockout.

6. CONCLUSIONS

The basic idea of the predictive controller represents an attractive method for minimization of the switching frequency in on-off controlled systems. As shown in this paper the problem lies in selecting the proper optimization criterion together with practicable constraints. Under consideration of an economical realization only a local optimization (according to a steepest descent method) is possible due to the simplicity of the mathematical conditions given in that case. This leads to a substantial improvement as compared to the simple hysteresis controller in such parameter regions where switching states can be assumed which have great influence on the variable to be optimized. (This means that the basic condition for good optimizability is given.) However, it is shown that in the case considered here the predictive controller does not justify the high effort of an on-line realization.

With a system being of much simpler structure, consisting basically of a switching table gained from off-line optimization, the selection of the "optimal" switching decision (according to the points of view mentioned) cannot be guaranteed in any case. However, this seeming disadvantage alltogether leads to a system behavior that - for an essential range of the parameters - lies closer to the global optimum than for the predictive controller. This is based on the fact that the predictive controller optimizes the system behavior only within a very limited

time interval. Therefore the optimum evaluated by the predictive controller is not the global optimum. It is shown that the proposed off-line optimized table based controller comes closer to the global optimum.

REFERENCES

[1] H.ERTL, J.W.KOLAR, F.C.ZACH: "Analysis of Different Current Control Concepts for Forced Commutated Rectifier (FCR)", in Proc. of the PCI Conf., 1986, Munich, pp.195-217

[2] J.HOLTZ, S.STADTFELD: "A PWM Inverter Drive System with On-line Optimized Pulse Patterns", in Proc. of the First European Conf. on Power Electronics and Applications, 1985, Brussels, vol.2, pp.3.21-3.25

ACKNOWLEDGEMENT

The authors are very much indebted to the Austrian "Fonds zur Förderung der wissenschaftlichen Forschung" who supports the work of the power electronics section at their university.